Chapter 25: Planar defects

Planar defects: orientation and types

Crystalline films often contain internal, 2-D interfaces separating two regions transformed with respect to one another, but with, otherwise, essentially, identical crystal structure. If the length scale of interest is large enough, the transformation relating the regions is usually isometric, meaning that distances and angles between equivalent points within the regions are unchanged. The interface represents a defect with respect to a perfect crystal. Locally, the interface is confined to a distinct 2-D plane. This may also be the case globally, so that the planar defect is truly confined to a plane over its entire extent. But there is a clear link to other types of 2-D, interfacial defects, which may spread over a non-planar, 2-D manifold, or membrane, so we will discuss these in the context of planar defect, too.

When observing these defects in TEM, we can expect two limiting cases for the local orientation of the planar defect: we may be viewing the defect either 1) parallel to its plane, which present transverse variations in the crystal potential w.r.t. the incident beam, or 2) perpendicular to its plane, in which case the variations are longitudinal.

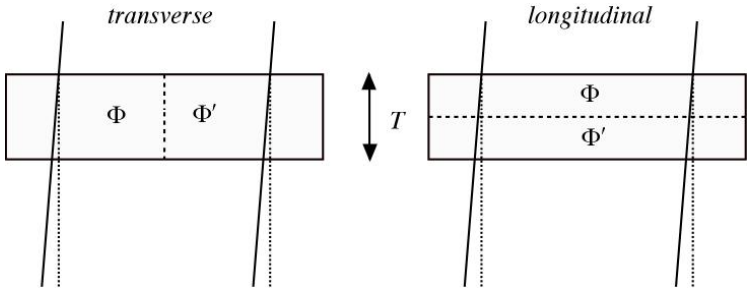

What types of isometric transformations are we talking about here? One common case is a translation by a displacement vector $\mathbf{R}$.

$$\Phi'(\mathbf{r}) = \Phi(\mathbf{r} - \mathbf{R})$$

Another possibility is a rotation or reflection, represented by a matrix $\tilde{\mathrm{M}}$.

$$\Phi'(\mathbf{r}) = \Phi\left(\tilde{\mathrm{M}}\mathbf{r}\right)$$

In the immediate vicinity of the planar defect, the potential could be quite complicated. But just a few unit cells or more away from the interface, the separate crystals should nearly resume their ideal, transformed structures. That's usually good enough to determine the type of defect that separates them.

Translation: Influence on Fourier coeff's

It is the change in crystal potential that influences the wave function of an electron propagating through the material that gives rise to any kind of image contrast or diffraction signature. Instead of $\Phi(\mathbf{r})$, electron diffraction mainly involves the structure function $U(\mathbf{r})$, or rather its Fourier components $U_{\mathbf{g}}$. For a translation, we expect

$$U'(\mathbf{r}) = U(\mathbf{r} - \mathbf{R})$$

Far from the defect, in the transformed region, we expect the crystal to be essentially perfect, so we can represent it by a Fourier series. For a translation, the RLVs needed are unchanged:

$$U'(\mathbf{r}) = \sum_{\mathbf{g}} U_{\mathbf{g}} e^{2\pi i \mathbf{g}\cdot(\mathbf{r}-\mathbf{R})} = \sum_{\mathbf{g}} \left(U_{\mathbf{g}} e^{-2\pi i \mathbf{g}\cdot\mathbf{R}}\right) e^{2\pi i \mathbf{g}\cdot\mathbf{r}} = \sum_{\mathbf{g}} U'_{\mathbf{g}} e^{2\pi i \mathbf{g}\cdot\mathbf{r}}$$

The only effect is a phase shift of some of the Fourier components:

$$U'_{\mathbf{g}} = U_{\mathbf{g}} e^{-2\pi i \mathbf{g}\cdot\mathbf{R}} = U_{\mathbf{g}} e^{i\alpha}$$

Notice that a component is only affected if $\mathbf{g}\cdot\mathbf{R} \neq 0$, that is, its RLV $\mathbf{g}$ has a component along $\mathbf{R}$. We can think of a general 2-D boundary, which may have an oblique orientation w.r.t. the incident beam, across which the some particular Fourier component has changed phase.

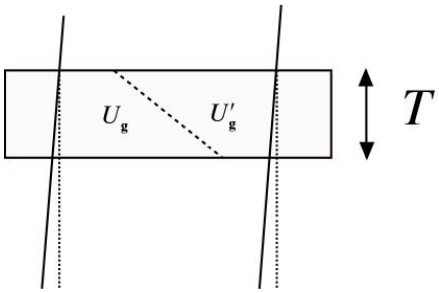

Different types of planar defects can give rise to various values of α. But a particularly easy case to analyze is when $\alpha = \pi$ for some reflection, so $U'_{\mathbf{g}} = -U_{\mathbf{g}}$. Though we assumed the transformation was a translation, the influence of a reflection or rotation on certain RLVs may be the same. In particular, we can associate this sign flip of certain Fourier components with antiphase boundaries (APBs). If we are only concerned with effect observed under a two-beam condition, a phase shift or change of sign of the active Fourier component may be all we need to analyze the diffraction and imaging effects.

Translation: influence on Bloch waves

Let's say we have the situation above. We have solved for the Bloch waves above the defect and find:

$$\psi^{(j)}(\mathbf{r}) = \left[\sum_{\mathbf{g}} C_{\mathbf{g}}^{(j)} e^{2\pi i \mathbf{g}\cdot\mathbf{r}}\right] \cdot e^{2\pi i \mathbf{k}^{(j)}\cdot\mathbf{r}}$$

Now let's find the solution below the defect. It's going to be the same as that above, except for the translation correspond to that of the crystal potential:

$$\begin{aligned}
\psi'^{(j)}(\mathbf{r}) &= \psi^{(j)}(\mathbf{r}-\mathbf{R}) \\
&= \left[\sum_{\mathbf{g}} C_{\mathbf{g}}^{(j)} e^{2\pi i \mathbf{g}\cdot(\mathbf{r}-\mathbf{R})}\right] \cdot e^{2\pi i \mathbf{k}^{(j)}\cdot(\mathbf{r}-\mathbf{R})} \\
&= \left[\sum_{\mathbf{g}} \left(C_{\mathbf{g}}^{(j)} e^{-2\pi i[\mathbf{g}+\mathbf{k}^{(j)}]\cdot\mathbf{R}}\right) e^{2\pi i \mathbf{g}\cdot\mathbf{r}}\right] \cdot e^{2\pi i \mathbf{k}^{(j)}\cdot\mathbf{r}} \\
\psi'^{(j)}(\mathbf{r}) &= \left[\sum_{\mathbf{g}} C'^{(j)}_{\mathbf{g}} e^{2\pi i \mathbf{g}\cdot\mathbf{r}}\right] \cdot e^{2\pi i \mathbf{k}^{(j)}\cdot\mathbf{r}}
\end{aligned}$$

The factor $\exp[-2\pi i \mathbf{k}^{(j)}\cdot\mathbf{R}]$ is common to every component of every Bloch wave, so we can just drop it and write

$$C'^{(j)}_{\mathbf{g}} = C_{\mathbf{g}}^{(j)} e^{-2\pi i \mathbf{g}\cdot\mathbf{R}} = C_{\mathbf{g}}^{(j)} e^{i\alpha}$$

As for the crystal potential, the only difference is a phase shift of some Fourier components of the Bloch waves: those for which $\mathbf{g}\cdot\mathbf{R} \neq 0$.

Scattering matrix (two-beam)

I'd like to predict the effects of a planar defect in oblique orientation in a two-beam condition, particularly the dark-field image contrast. If the defect only causes a phase shift in the Fourier coefficient of the active reflection g, we can start with our dynamical theory from before. Since we already know how to do that problem, let's boil it down to its basics. The two-beam result can be summarized in matrices as:

$$\begin{pmatrix}\Psi_{\mathbf{0}}(z)\\ \Psi_{\mathbf{g}}(z)\end{pmatrix}=\begin{pmatrix}C_{\mathbf{0}}^{(1)} & C_{\mathbf{0}}^{(2)}\\ C_{\mathbf{g}}^{(1)} & C_{\mathbf{g}}^{(2)}\end{pmatrix}\cdot\begin{pmatrix}e^{2\pi i\gamma^{(1)}z} & 0\\ 0 & e^{2\pi i\gamma^{(2)}z}\end{pmatrix}\cdot\begin{pmatrix}\varepsilon^{(1)}\\ \varepsilon^{(2)}\end{pmatrix}=\tilde{C}\cdot\tilde{\Gamma}(z)\cdot\begin{pmatrix}\varepsilon^{(1)}\\ \varepsilon^{(2)}\end{pmatrix}$$

This gives us the diffracted amplitudes at some depth z. We know that at the entrance surface:

$$\begin{pmatrix}\Psi_{\mathbf{0}}(0)\\ \Psi_{\mathbf{g}}(0)\end{pmatrix}=\tilde{C}\cdot\begin{pmatrix}\varepsilon^{(1)}\\ \varepsilon^{(2)}\end{pmatrix}$$

so we can find the excitation amplitudes using

$$\begin{pmatrix}\varepsilon^{(1)}\\ \varepsilon^{(2)}\end{pmatrix}=(\tilde{C})^{-1}\cdot\begin{pmatrix}\Psi_{\mathbf{0}}(0)\\ \Psi_{\mathbf{g}}(0)\end{pmatrix}$$

Now we have

$$\begin{pmatrix}\Psi_{\mathbf{0}}(z)\\ \Psi_{\mathbf{g}}(z)\end{pmatrix}=\tilde{C}\cdot\tilde{\Gamma}(z)\cdot(\tilde{C})^{-1}\cdot\begin{pmatrix}\Psi_{\mathbf{0}}(0)\\ \Psi_{\mathbf{g}}(0)\end{pmatrix}$$

Let's combine the product of matrices into one 2 x 2 matrix, called the scattering matrix:

$$\tilde{P}(z)=\tilde{C}\cdot\tilde{\Gamma}(z)\cdot\tilde{C}^{-1}$$

which gives

$$\begin{pmatrix}\Psi_{\mathbf{0}}(z)\\ \Psi_{\mathbf{g}}(z)\end{pmatrix}=\tilde{P}(z)\cdot\begin{pmatrix}\Psi_{\mathbf{0}}(0)\\ \Psi_{\mathbf{g}}(0)\end{pmatrix}$$

Propagation across a planar defect (I)

Below the planar defect (fault) we described previously, at a depth $z=t$ from the entrance surface, we have

$$\begin{pmatrix}\Psi'_{\mathbf{0}}(z)\\ \Psi'_{\mathbf{g}}(z)\end{pmatrix}=\tilde{C}'\cdot\tilde{\Gamma}'(z-t)\cdot\begin{pmatrix}\varepsilon'^{(1)}\\ \varepsilon'^{(2)}\end{pmatrix}$$

Interestingly, the eigenvalues are the same as above the fault. It is only the Bloch-wave coefficients that have changed

$$\tilde{C}'=\begin{pmatrix}1 & 0\\ 0 & e^{-i\alpha}\end{pmatrix}\cdot\tilde{C}$$

As before, we have

$$\begin{pmatrix}\Psi'_{\mathbf{0}}(t)\\ \Psi'_{\mathbf{g}}(t)\end{pmatrix}=\tilde{C}'\cdot\begin{pmatrix}\varepsilon'^{(1)}\\ \varepsilon'^{(2)}\end{pmatrix}$$

so

$$\begin{pmatrix}\varepsilon'^{(1)}\\ \varepsilon'^{(2)}\end{pmatrix}=(\tilde{C}')^{-1}\cdot\begin{pmatrix}\Psi'_{\mathbf{0}}(t)\\ \Psi'_{\mathbf{g}}(t)\end{pmatrix}$$

The scattering matrix in this region is

$$\tilde{P}'(z-t)=\tilde{C}'\cdot\tilde{\Gamma}'(z-t)\cdot(\tilde{C}')^{-1}$$

which allows us to write

$$\begin{pmatrix}\Psi'_{\mathbf{0}}(z)\\ \Psi'_{\mathbf{g}}(z)\end{pmatrix}=\tilde{P}'(z-t)\cdot\begin{pmatrix}\Psi'_{\mathbf{0}}(t)\\ \Psi'_{\mathbf{g}}(t)\end{pmatrix}$$

Propagation across a planar defect (II)

The key ingredient is the boundary conditions at the planar defect. It is usually sufficient to only require that continuity of the wave function

$$\begin{pmatrix}\Psi'_{\mathbf{0}}(t)\\ \Psi'_{\mathbf{g}}(t)\end{pmatrix}=\begin{pmatrix}\Psi_{\mathbf{0}}(t)\\ \Psi_{\mathbf{g}}(t)\end{pmatrix}$$

Now the wave function below the fault is

$$\begin{pmatrix}\Psi'_{\mathbf{0}}(z)\\ \Psi'_{\mathbf{g}}(z)\end{pmatrix}=\tilde{P}'(z-t)\cdot\tilde{P}(t)\cdot\begin{pmatrix}\Psi_{\mathbf{0}}(0)\\ \Psi_{\mathbf{g}}(0)\end{pmatrix}$$

In fact, the boundary condition at the entrance surface of the foil also tells us that $\Psi_{\mathbf{0}}(0)=1$ and $\Psi_{g}(0)=0$, so life just gets easier and easier. At the exit surface of the foil ($z=T$)

$$\begin{pmatrix}\Psi'_{\mathbf{0}}(T)\\ \Psi'_{\mathbf{g}}(T)\end{pmatrix}=\tilde{P}'(T-t)\cdot\tilde{P}(t)\cdot\begin{pmatrix}1\\ 0\end{pmatrix}$$

Antiphase boundary

APBs are probably the simplest type of planar defect, allowing us to test our understanding of how electrons propagate across such defects. Imagine a 1:1 alloy with random substitution of the two components on lattice sites. Now assume some ordering of these components, with the type of atom alternating periodically in some direction (a superlattice). Ordering has also occurred in some other part of the crystal, but with the two atoms exchanged in the ordering sequence – a so-called antiphase domain. Where these two regions occur, we have an APB.

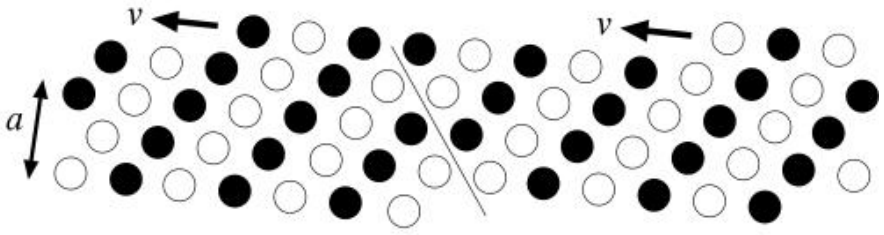

Say the structure factor for a superlattice reflection on one side of the boundary is $F_{\mathbf{g}} = f_A - f_B$. On the other side, it will be $F'_{\mathbf{g}} = f_B - f_A = -F_{\mathbf{g}}$.

Propagation across an APB (I)
The eigenvalue matrix can be written

$$\Gamma(z) = \mathrm{e}^{\pi i w z/\xi} \cdot \begin{pmatrix} \mathrm{e}^{\pi i \sqrt{1+w^2}\, z/\xi} & 0 \\ 0 & \mathrm{e}^{-\pi i \sqrt{1+w^2}\, z/\xi} \end{pmatrix}$$

in terms of $w = 1/s\xi$. The Bloch-wave coefficients in a two-beam condition can be written

$$\tilde{\mathrm{C}} = \begin{pmatrix} \sin(\beta/2) & -\cos(\beta/2) \\ \cos(\beta/2) & \sin(\beta/2) \end{pmatrix}$$

where

$$\sin(\beta) = 1/\sqrt{1+w^2} \text{ and } \cos(\beta) = w/\sqrt{1+w^2}$$

We will need to find the scattering matrix

$$\tilde{\mathrm{P}}(z) = \tilde{\mathrm{C}} \cdot \tilde{\Gamma}(z) \cdot \tilde{\mathrm{C}}^{-1}$$

Then, below the fault, we have

$$\tilde{\mathrm{C}}' = \begin{pmatrix} 1 & 0 \\ 0 & -1 \end{pmatrix} \cdot \tilde{\mathrm{C}} = \begin{pmatrix} \sin(\beta/2) & -\cos(\beta/2) \\ -\cos(\beta/2) & -\sin(\beta/2) \end{pmatrix}$$

Then we can find

$$\tilde{\mathrm{P}}'(z-t) = \tilde{\mathrm{C}}' \cdot \tilde{\Gamma}'(z-t) \cdot (\tilde{\mathrm{C}}')^{-1}$$

Propagation across an APB (II)
Let's simplify some more by considering the strong beam case ($s = 0$). Now $\gamma^{(1,2)} = \pm 1/2\xi$

$$\Gamma(z) = \begin{pmatrix} \mathrm{e}^{\pi i z/\xi} & 0 \\ 0 & \mathrm{e}^{-\pi i z/\xi} \end{pmatrix}$$

and

$$\tilde{C} = \frac{1}{\sqrt{2}}\begin{pmatrix} 1 & -1 \\ 1 & 1 \end{pmatrix};\ \tilde{C}' = \frac{1}{\sqrt{2}}\begin{pmatrix} 1 & -1 \\ -1 & -1 \end{pmatrix}$$

Let's define $a = \pi t/\xi$ and $b = \pi T/\xi$. Now

$$\tilde{\Gamma}(t) = \begin{pmatrix} e^{ia} & 0 \\ 0 & e^{-ia} \end{pmatrix} \text{ and } \tilde{\Gamma}(T-t) = \begin{pmatrix} e^{i(b-a)} & 0 \\ 0 & e^{-i(b-a)} \end{pmatrix}$$

First

$$\tilde{P}(t) = \frac{1}{2}\begin{pmatrix} 1 & -1 \\ 1 & 1 \end{pmatrix} \cdot \begin{pmatrix} e^{ia} & 0 \\ 0 & e^{-ia} \end{pmatrix} \cdot \begin{pmatrix} 1 & 1 \\ -1 & 1 \end{pmatrix} = \begin{pmatrix} \cos(a) & i\sin(a) \\ i\sin(a) & \cos(a) \end{pmatrix}$$

Next

$$\tilde{P}'(T-t) = \frac{1}{2}\begin{pmatrix} 1 & -1 \\ -1 & -1 \end{pmatrix} \cdot \begin{pmatrix} e^{i(b-a)} & 0 \\ 0 & e^{-i(b-a)} \end{pmatrix} \cdot \begin{pmatrix} 1 & -1 \\ -1 & -1 \end{pmatrix} = \begin{pmatrix} \cos(b-a) & -i\sin(b-a) \\ -i\sin(b-a) & \cos(b-a) \end{pmatrix}$$

Propagation across an APB (III)

Now applying the boundary condition at the entrance surface:

$$\tilde{P}(t) \cdot \begin{pmatrix} 1 \\ 0 \end{pmatrix} = \begin{pmatrix} \cos(a) \\ i\sin(a) \end{pmatrix}$$

Putting this all together

$$\tilde{P}(T-t) \cdot \tilde{P}(t) \cdot \begin{pmatrix} 1 \\ 0 \end{pmatrix} = \begin{pmatrix} \cos(b-a) & -i\sin(b-a) \\ -i\sin(b-a) & \cos(b-a) \end{pmatrix} \cdot \begin{pmatrix} \cos(a) \\ i\sin(a) \end{pmatrix} = \begin{pmatrix} \cos(2a-b) \\ i\sin(2a-b) \end{pmatrix}$$

We finally have

$$\begin{pmatrix} \Psi_0'(T) \\ \Psi_g'(T) \end{pmatrix} = \begin{pmatrix} \cos[\pi(2t-T)/\xi] \\ i\sin[\pi(2t-T)/\xi] \end{pmatrix}$$

Diffracted intensity across an APB

We can look at this result as a variation in intensity of the diffracted beam as the electron propagates through the foil. Above the APB, the diffracted intensity is

$$|\Psi_g(z)|^2 = \sin^2(\pi z/\xi)$$

Below the APB, we have

$$|\Psi_g'(z)|^2 = \sin^2[\pi(2t-z)/\xi]$$

The derivative dI_g/dz reverses at the APB. If the APB is at $t = T/2$, the image intensity for the APB is always dark, regardless of T.

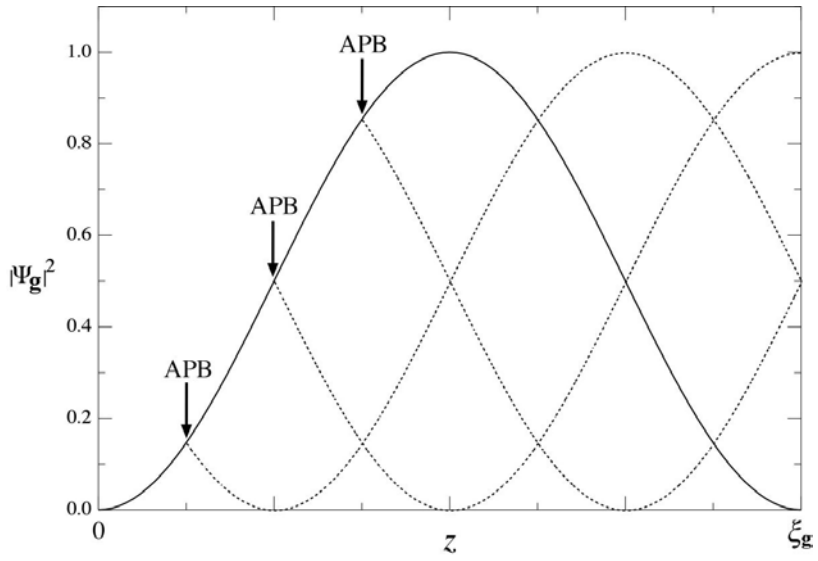

DF images of inclined APBs: influence of tilt

If we set up a sample with APBs at the Bragg condition and using DF imaging with a reflection that is sensitive to the phase, the APBs do, indeed, appear dark with respect to the surrounding material. Tilting slightly away from the Bragg condition also gives some interesting image contrast. First, the contrast reverses, so the APBs appear bright on a dark background. A little more tilt causes the APB to show two bright fringes on a dark background.

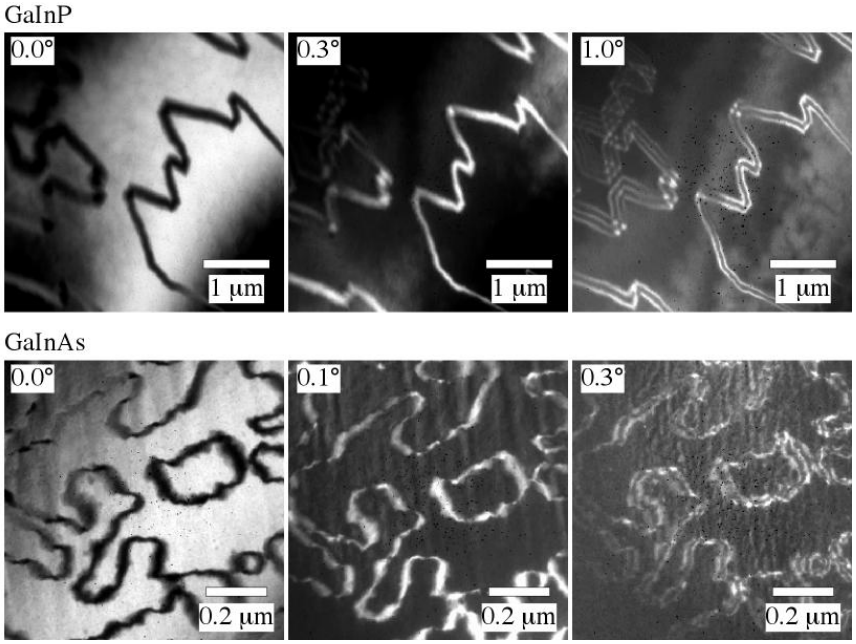

Inclined APBs: two-beam analysis

The general two-beam case takes a bit more work. From the form of the eigenvalues

$$\gamma^{(1,2)} = \left(w \pm \sqrt{w^2+1}\right)/2\xi$$

we might guess that something interesting happens when $\omega^2 + 1 = N^2$, where N is an integer. There is no need to work these out analytically every time; the problem is ideally suited for a computer.

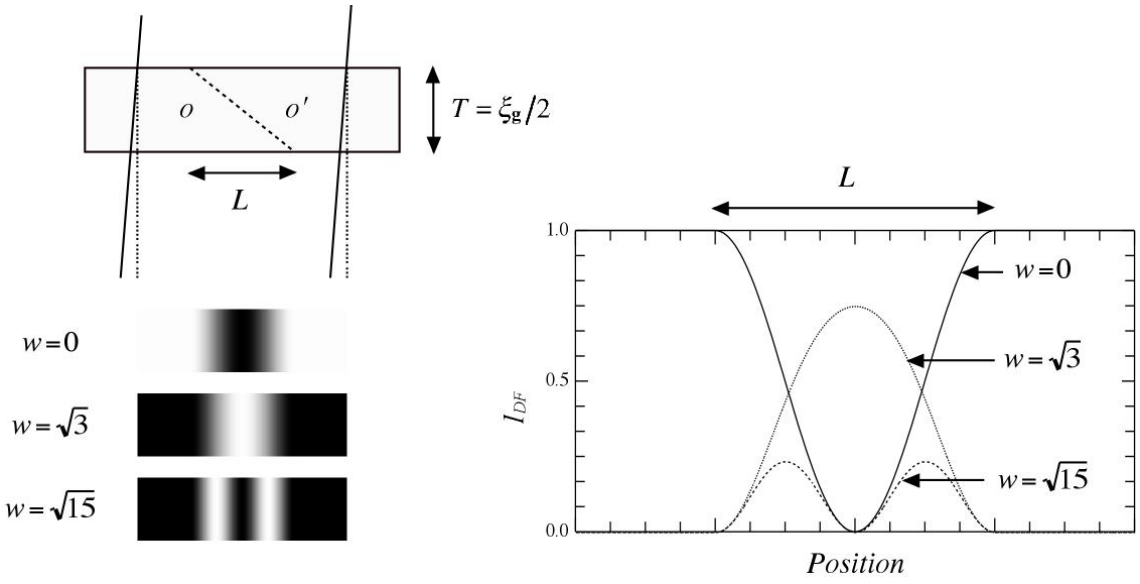

The calculations match what was observed experimentally.

Stacking faults in fcc crystals

Stacking faults involve an extra or missing plane in the stacking sequence of a crystal. We saw that the {111} planes play a special role in fcc materials. Say we label the normal stacking sequence as ABCABCA… We can imagine removing a plane - C, for example - from the whole sample, or just a portion of the sample. Then the stacking sequence in that region is ABABCA… This is an intrinsic stacking fault.

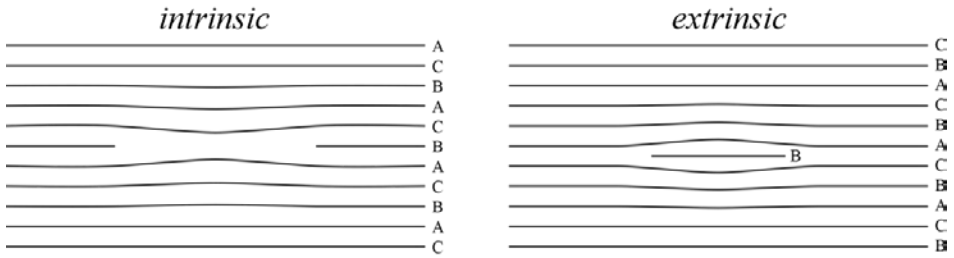

If, instead, we insert an extra plane in some region, ABCBABC…, then we have an extrinsic stacking fault.

Stacking fault geometry

The linear boundaries of a stacking fault have some of the qualities of dislocations. But since we can't draw a Burger's circuit through a surrounding region of perfect material, they are called "partial" dislocations.

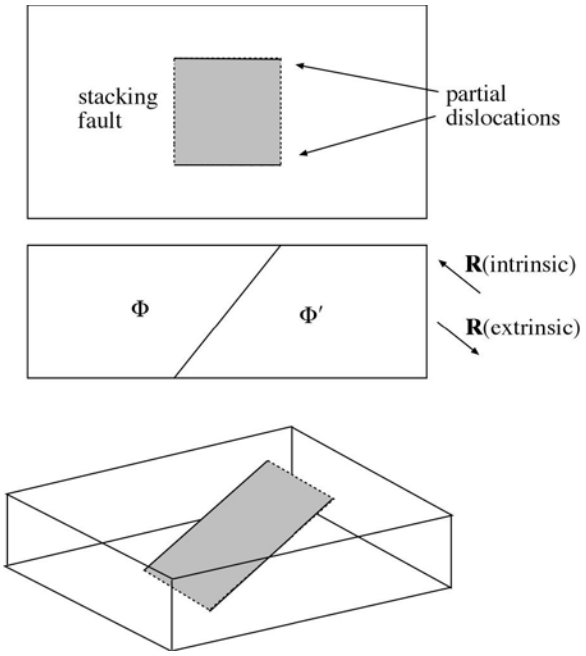

In [001]-oriented semiconductor films, the {111} planes are inclined from the interface. We can think the corresponding translation vector $\mathbf{R}$ for intrinsic and extrinsic stacking faults as being in opposite directions, though the choice will depend on whether we consider $\mathbf{R}$ to be $\langle 111\rangle/3$ or $2\langle 111\rangle/3$.

Stacking fault images

To view stacking faults in TEM DF images, we need to use a RLV for which $\mathbf{g}\cdot\mathbf{R}\neq 0$. If we use a reflection having $\mathbf{g}\cdot\mathbf{R}=0$, we may see that partial dislocations bordering the SF, but get no contrast from the SF itself. If we do have $\mathbf{g}\cdot\mathbf{R}\neq 0$, fringes become appear along the SF. The fringe spacing depends on the foil thickness.

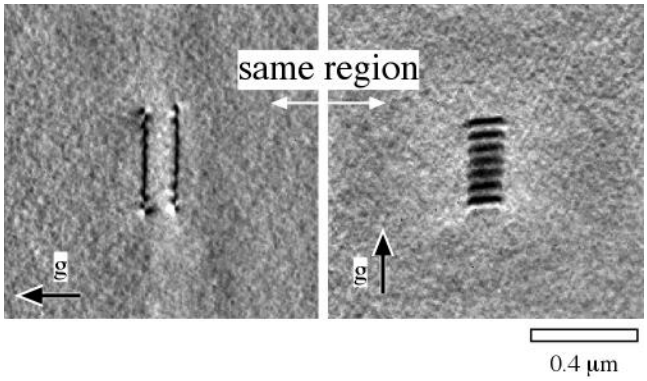

Twin boundaries in fcc crystals

A common type of planar defect that arises in fcc crystals is twinning. The stacking configuration of <111> planes in fcc is closely linked to [0001] stacking in hcp, because the energy difference is usually fairly small. Sometime, so-called “microtwins” form that just span a few unit cells in width. The twin domains will share {111} planes with the matrix regions.

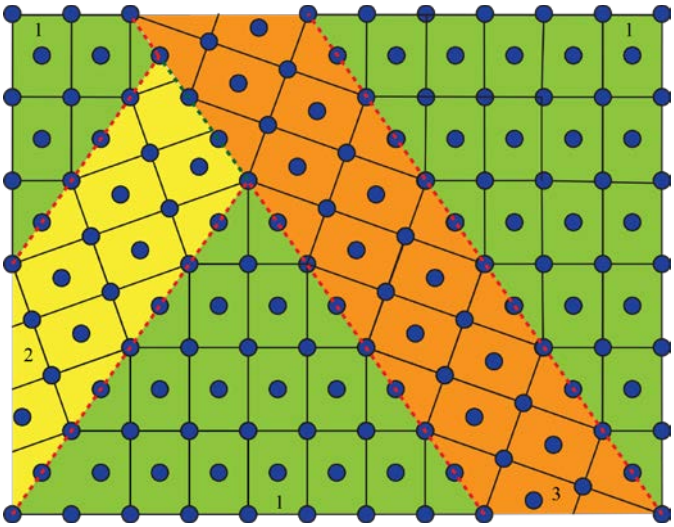

The signature of twins in fcc crystals is extra diffraction spots at $(111)/3$ and equivalent positions. These are especially evident on <110> zone axes, where two sets of {111} diffraction spots appear, which can each present transverse twin boundaries. Using the extra spots for DF imaging highlights domains of the twinned area, which may be embedded in matrix with a single, dominant orientation.

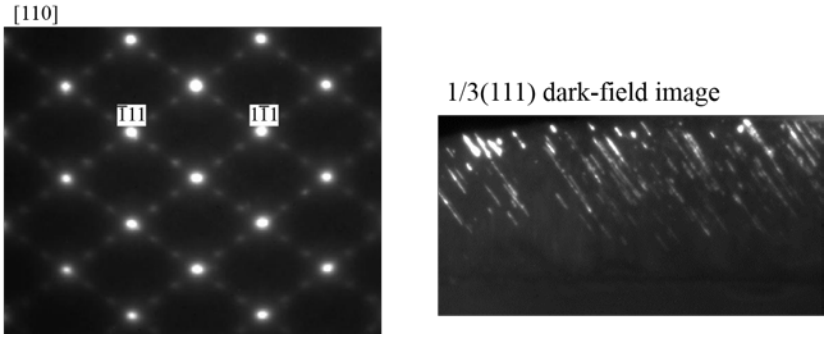

Origin of 1/3{111} position spots

Start with the matrix spots in a [110] diffraction pattern of a zincblende (fcc) crystal.

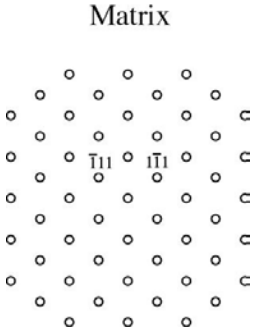

In 2-D projection, a rotation by 180° about $(\bar{1}11)$ is equivalent to a reflection across $(1\bar{1}2)$. Likewise, a rotation by 180° about $(1\bar{1}1)$ is equivalent to a reflection across $(\bar{1}12)$. A little bookkeeping shows that the extra spots combine with the original pattern at 1/3{111} positions.

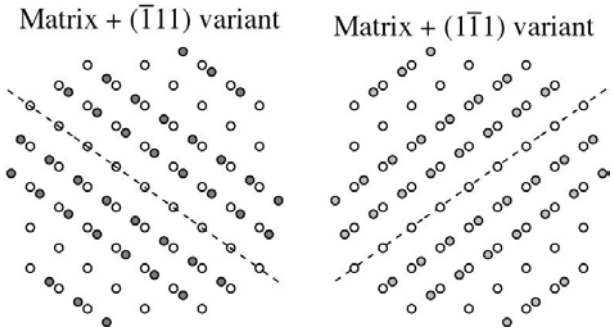

We don't immediately get all of the spots seen in the experimental pattern, though. Dynamical diffraction is needed to generate the entire pattern.